Spectroscopic Properties of Nanotube–Chromophore Hybrids

Changshui Huang,[†] Randy K. Wang,[‡] Bryan M. Wong,[⊥] David J. McGee,[∥] François Léonard,[⊥] Yun Jun Kim,[†] Kirsten F. Johnson,[†] Michael S. Arnold,[†] Mark A. Eriksson,[‡,*] and Padma Gopalan[†,§,*]

[†]Department of Materials Science & Engineering, [‡]Department of Physics, and [§]Department of Chemistry, University of Wisconsin—Madison, Madison, Wisconsin 53706, United States, [⊥]Sandia National Laboratories, Livermore, California 94551, United States, and [∥]Department of Physics, The College of New Jersey, Ewing, New Jersey 08628, United States

ABSTRACT Recently, individual single-walled carbon nanotubes (SWNTs) functionalized with azo-benzene chromophores were shown to form a new class of hybrid nanomaterials for optoelectronics applications. Here we use a number of experimental and computational techniques to understand the binding, orientation, and nature of coupling between chromophores and the nanotubes, all of which are relevant to future optimization of these hybrid materials. We find that the binding energy between chromophores and nanotubes depends strongly on the type of tether that is used to bind the chromophores to the nanotubes. The pyrene tethers form a much stronger attachment to nanotubes compared to anthracene or benzene rings, resulting in more than 80% retention of bound chromophores post-processing. Density functional theory (DFT) calculations show that the binding energy of the chromophores to the nanotubes is maximized for chromophores parallel to the nanotube sidewall, even with the use of tethers; optical second harmonic generation measurements show that there is nonetheless a partial radial orientation of the chromophores on the nanotubes. We find weak electronic coupling between the chromophores and the SWNTs, consistent with noncovalent binding. This weak coupling is still sufficient to quench the chromophore fluorescence through a combination of static and dynamic processes. Photoluminescence measurements show a lack of significant energy transfer from the chromophores to isolated semiconducting nanotubes.

KEYWORDS: azo-benzene chromophore · single-walled carbon nanotubes · binding · orientation · quenching

Light-triggered changes in biological molecules, which enable various functions such as vision,[1] photosynthesis, and heliotropism,[2] have long inspired materials chemists to mimic these phenomena to create new synthetic materials and devices. One example is the molecule retinal undergoing a *cis*–*trans* isomerization in response to light,[3] creating a cascade of events leading to visual recognition.[4] Synthetic versions of retinal include switchable stilbene or azo-benzene-containing molecules. Azo-benzenes undergo a reversible photoisomerization from a thermally stable *trans* configuration to a metastable *cis* form. Dipolar chromophores based on the azo-benzene structure are photochemically stable, can be reversibly switched 10^5 to 10^6 times before bleaching, and can be chemically tuned at the donor and acceptor end to alter the magnitude of the dipole moment.[5] The *cis*–*trans* isomerization of a range of chromophores has been studied extensively in solution and as monolayers on gold-coated flat substrates[6] or on silicon substrates using scanning tunneling microscopy (STM).[7,8] Hence, azo-benzene chromophores constitute a well-understood switching unit for attachment to nanotubes to create new hybrid materials. The reversible, wavelength-selective isomerization and the accompanying conformational change provides an important handle for optical modulation of electrical and electro-optic properties of nanotubes. We recently demonstrated an optically active nanotube hybrid material by noncovalent functionalization of SWNT field-effect transistors with an azo-based chromophore.[9] Upon UV illumination, the chromophore undergoes a *trans*–*cis* isomerization leading to charge redistribution near the nanotube. The resulting change in the local electrostatic environment leads to a shift in the threshold voltage and increased conductivity of the nanotube. The functionalized transistors showed repeatable switching for many cycles, and the low (100 μW/cm^2) intensities necessary to optically modulate the transistor are in stark contrast to measurements of intrinsic nanotube photoconductivity, which typically require 1 kW/cm^2 intensity.[10] Subsequently, this approach was extended to demonstrate photodetection with tunability over the visible range by changing the chromophore structure.[11] More recently, it was proposed that chromophores/nanotube hybrids could serve as efficient energy storage materials.[12] There have been other approaches based on covalent functionalization of multiwalled nanotubes,[13,14] as well as azo-benzene-containing polymers wrapped on nanotubes, focusing mainly on *cis*–*trans* isomerization dynamics.[15]

* Address correspondence to pgopalan@cae.wisc.edu, maeriksson@wisc.edu.

Received for review March 24, 2011 and accepted September 15, 2011.

Published online September 15, 2011
10.1021/nn202725g

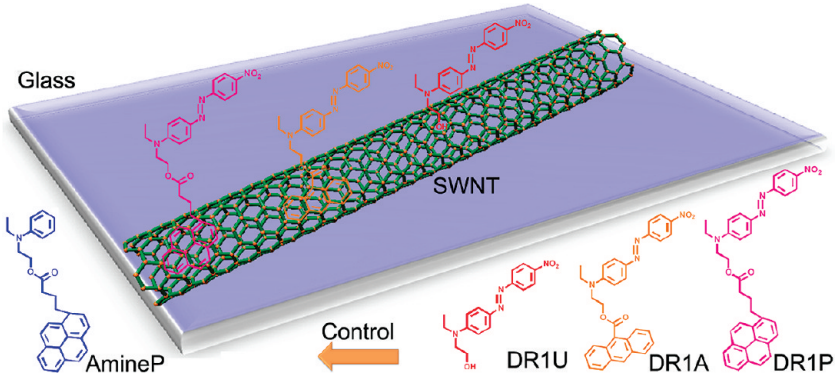

Scheme 1. Depiction of the SWNT hybrid along with the structures of unmodified DR1 (DR1U), DR1 with anthracene tether (DR1A), DR1 with pyrene (DR1P) tether, and the control compound, which is a pyrene tether on the donor amine group (AmineP).

In order to improve the efficiency, stability, and lifetime of chromophore-functionalized SWNT devices, it is important to understand the chromophore/SWNT interactions, including the role of tethers in binding the chromophores to the SWNTs. In this paper, we report the spectroscopic analysis of SWNT–azo-benzene chromophore hybrid systems using complementary experimental techniques and *ab initio* calculations. For the chromophore, we use Disperse Red 1 (DR1), a well-studied and commercially available azo-benzene chromophore (pseudo-stilbene-type azo compound), with a series of three increasing tether strengths: (1) unmodified DR1 with no added tether (DR1U), (2) anthracene-functionalized DR1 (DR1A), and (3) pyrene-functionalized DR1 (DR1P) (see Scheme 1). The first part of our studies on thin films shows that the binding energy and hence the surface coverage of the chromophores on the nanotubes is strongly influenced by the strength of the tether; we also address the question of the orientation of the molecules on the nanotubes by optical second harmonic generation (SHG) measurements. The second part of our studies focuses on the solution characterization of the hybrids to evaluate the nature of the electronic coupling. We find weak electronic coupling between the chromophores and the SWNTs, consistent with noncovalent binding, as verified by *ab initio* calculations. Our experiments show strong fluorescence quenching of the chromophores upon binding to the SWNTs and indicate that both static and dynamic quenching mechanisms are present.

RESULTS AND DISCUSSION

Evaluation of the Strength of Binding. SWNTs can interact with a DR1 unit by $\pi-\pi$ stacking interactions with the two benzene rings and/or by $\pi-\pi$ stacking interactions with anthracene and pyrene tethers, if present.[16−18] However, the strength of binding and the resulting surface coverage can vary greatly, and both are relevant for the fabrication of useful devices.

Raman spectroscopy was used to characterize the SWNT–chromophore hybrids, as it allows the measurement of vibrational modes of both the chromophores and the SWNTs. Raman spectra were collected in the 1200 to 1800 cm^{-1} range following excitation with a 532 nm laser (Figure 1A–D). Raman spectra of SWNTs typically consist of a graphitic or G-band[19] from highly ordered sidewalls, while disorder in the sidewall structure results in the D-band. From the Raman spectra (orange line) of pristine SWNTs, the D-band is observed in the region of 1300–1350 cm^{-1} and the G-band in the 1500–1650 cm^{-1} range. The asymmetric shoulder at 1540 cm^{-1} on the G-band is due to electron–phonon coupling in bundles of SWNTs.[20] The Raman spectra of the hybrids show the characteristic peaks from DR1 in the 1200–1600 cm^{-1} range (see Supporting Information Figure 1S). When compared to the pristine SWNTs, the hybrids show the following changes: (1) an increased peak intensity at ~1330 cm^{-1}, due to contributions from the N–O and C–N stretching vibrations of the chromophore; (2) the appearance of new peaks around 1350–1500 cm^{-1} attributed to N=N, $C_{ph}-N_{Me}$, and C–C stretching vibrations and C–C and C–N in-plane bending vibrations of the chromophore;[21,22] and (3) increased intensity of the peak at 1500–1550 cm^{-1} due to contributions from the C–C stretching vibrations from the chromophores. Hence, quantitative comparison of the peak intensities in the 1200–1800 cm^{-1} range can give us an estimate of the amount of bound chromophore. Upon washing the DR1U/SWNT (Figure 1A) hybrid with methanol to remove any weakly bound molecules, the intensity of the characteristic peaks from the chromophores (region A_1 in Figure 1) decreased significantly (region A_2 in Figure 1). In contrast, the peaks in the DR1P/SWNT showed a less significant decrease, as shown in Figure 1C. The information from Figure 1A–C is summarized in Figure 1D as a plot of the relative binding efficiencies of the three types of bound molecules to nanotubes. Comparison of the normalized area before and after methanol washing shows retention of 30, 40, and 60% of DR1U, DR1A, and DR1P, respectively. A

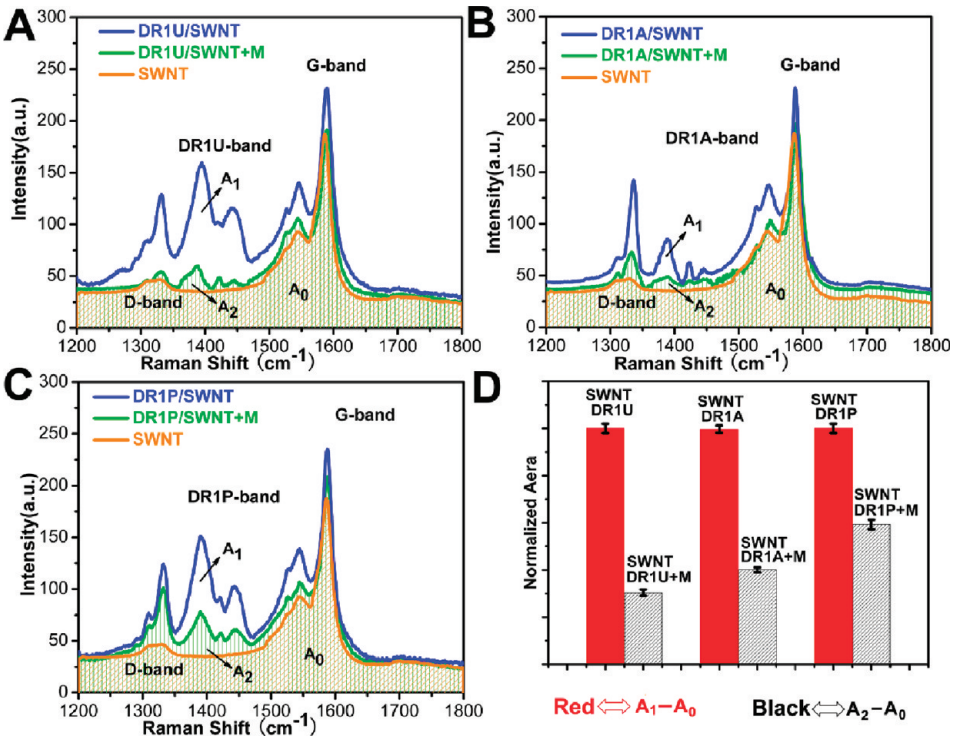

Figure 1. (A−C) Raman spectra of SWNTs (orange), chromophore−SWNT hybrids (blue), and the same hybrids after washing with methanol (green) for DR1U, DR1A, and DR1P, respectively. (D) Quantitative assessment of the normalized efficiency of binding for DR1U, DR1A, and DR1P. Red bars correspond to the intensity from the bound chromophores [difference in the peak areas represented by A_1 (intensity after binding the chromophores to SWNTs) and A_0 (intensity from the bare nanotubes)]; and the gray bars correspond to the intensity from the bound chromophores remaining after methanol wash [the difference in the peak areas represented by A_2 (intensity after washing the chromophore bound SWNTs with methanol) and A_0 (intensity from the bare nanotubes)].

similar analysis performed by UV−vis spectroscopy shows up to 80% retention of chromophores when a pyrene tether is present (details in Figure 2S). These results confirm the importance of a strongly $\pi-\pi$ interacting group such as pyrene in the formation of a more stable structure compared to stacking by benzene rings or anthracene units.

X-ray photoelectron spectroscopy (XPS) provides another means to probe the surface chemical composition and to evaluate the surface coverage. Figure 2A shows the N (1s) XPS spectra of nanohybrid films. After washing with methanol, the decrease in the N (1s) peak intensity was in the order DR1U/SWNTs > DR1A/SWNTs > DR1P/SWNTs. The following bonds were assigned (Figure 2B,C) as follows: N═N (397.38−401.53 eV), N−C (398.28−403.53 eV), NO_2 (403.18−408.29 eV); sp^2 C═C and sp^3 C−C (282.38−286.21 eV), C−O (283.91−287.19 eV), C−N (283−287.5 eV), >C═O (285.21−287.98 eV), −COO and O−COO (286.52−289.09 eV), $\pi-\pi^*$ transitions associated with phenyl rings (288.51−291.1 eV).[23] The N (1s) peak around 400.3 eV has contributions from the azo, nitro, and amine groups on the chromophore. The C (1s) peak centered at 284 eV has contributions from both the carbon atoms in the chromophore and the SWNTs. The ratio of nitrogen atoms to nanotube carbon atoms was calculated from the XPS spectra (Figure 2D). The calculated coverages are 0.64, 0.67, and 3.12 molecules per 100 nanotube carbon atoms for DR1U/SWNTs, DR1A/SWNTs, and DR1P/SWNTs hybrids, respectively. After the hybrids were washed with methanol, the differences between these three systems are dramatic. The surface coverage of DR1U and DR1A on nanotubes decreased by 78 and 76%, respectively, whereas that of DR1P decreased by only 10%. These results are in agreement with the Raman and UV−vis data discussed earlier and confirm that the pyrene tether plays an important role in forming stable nanotube hybrids.

These experimental results can be compared with theoretical predictions of binding energies and electronic structures of the various chromophore−SWNT hybrids using all-electron *ab initio* calculations.[24,25] In these calculations, the binding energies are affected by the geometrical orientation of the chromophore on the nanotube. Figure 3 shows the relaxed atomic structures and electronic band structures for three configurations: (a) DR1U, (b) DR1P perpendicular to the SWNT axis, and (c) DR1P parallel to the SWNT axis. These calculations indicate that DR1P in the parallel configuration (1.55 eV) shows a stronger binding interaction to SWNTs than DR1U (0.79 eV), while the perpendicular configuration of DR1P (0.64 eV) has a smaller binding energy as DR1U. (It is worth noting that the binding energy of DR1P in the parallel configuration is roughly

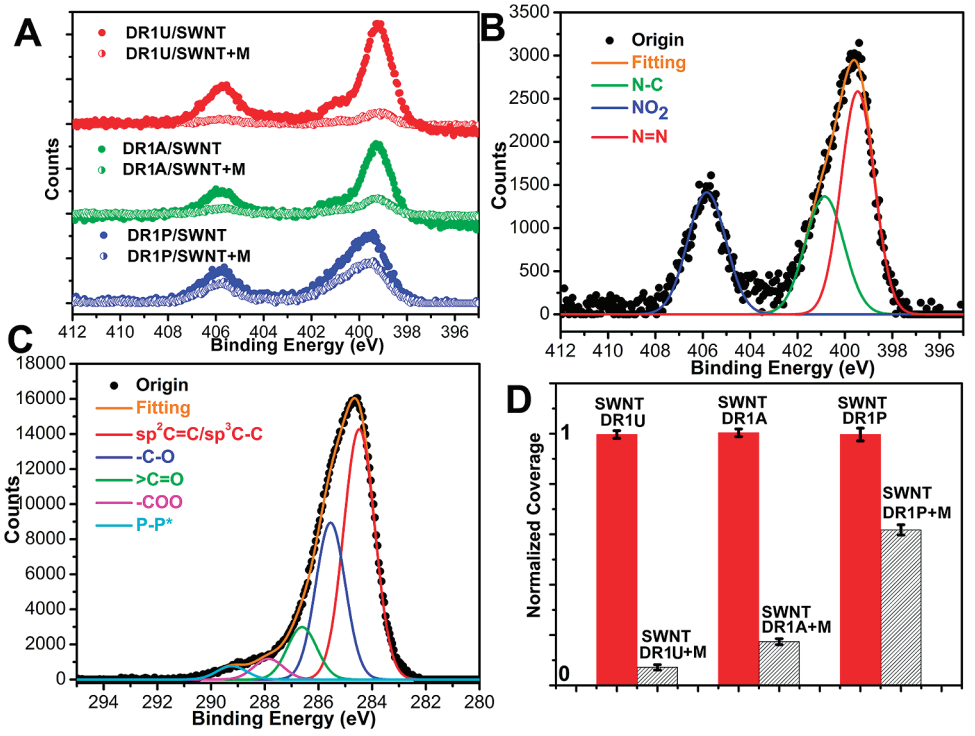

Figure 2. XPS spectra of chromophore−SWNT films showing (A) XPS core level N (1s) spectra for the three nanohybrid films as cast and after methanol washing, (B) N (1s) spectra of the DR1P/SWNT hybrid with the fitting, (C) C (1s) spectra of DR1P/SWNT hybrid with the fitting, and (D) normalized surface coverage of chromophores on SWNTs calculated by comparison of the area under the N (1s) peak with the area under the C (1s) peak. Red bars correspond to the coverage of the chromophores on the substrate before washing (which is set to 1), and the gray bars correspond to the coverage of the chromophores bound to the nanotubes after methanol rinse.

equal to the sum of the energies of DR1U and of DR1P in the perpendicular orientation.) In all three systems, the nanotube electronic properties near the band gap are not strongly affected. As shown in Figure 3, the valence and conduction bands of the nanotube shift, but they do so together, with very little change in the band gap. Further, the chromophore energy levels near the HOMO and LUMO do not hybridize with the nanotube band structure. Moving above the LUMO or below the HOMO, a small degree of hybridization between the SWNT and chromophore levels is seen. Overall, the DFT calculations indicate that there is weak but nonzero electronic coupling between the chromophore and the nanotube, consistent with the small shifts observed in the G-band in the Raman spectra (Figure 3S in the Supporting Information).

According to the experimental UV spectra, Raman spectra, and XPS, DR1P shows stronger interaction to the nanotubes than DR1U, which suggests that at least some parallel orientation of DR1P is present in the experimental samples. However, if the binding of chromophores to nanotubes was entirely parallel to the surface, it would require re-examining the mechanism of gating of phototransistors,[9,11] which was explained based on a perpendicular orientation of the chromophores on the SWNTs. Such a parallel orientation would result in a macroscopically symmetric system with no net orientation of dipoles, so that no change would be observed in electrostatic potential around the nanotubes when the hybrids are exposed to light. To understand chromophore orientation in more detail, we performed optical second harmonic generation experiments on the nanotube hybrids both in the as-cast form and upon UV illumination.

Second harmonic generation (SHG) has proven to be a sensitive probe for the determination of acentric molecular ordering in monolayers and thin film,[26,27] and which to our knowledge has not been applied to the study of chromophore-functionalized nanotubes. As described below, we have utilized SHG to identify a radial component of chromophore orientation with respect to the SWNT surface.[28,29] When irradiated by a laser pulse, a collection of weakly interacting chromophores will generate a second harmonic pulse, with an intensity that depends on the molecular second-order hyperpolarizability β and a macroscopic order parameter describing the average orientation of a chromophore with respect to an axis of symmetry (in this case, normal to the SWNT film). Since isomerization of DR1 results in an approximate 5-fold decrease in β in going from the *trans* to the *cis* conformation,[28] monitoring SHG emission from the SWNT−chromophore hybrid during UV exposure should provide insight on the net chromophore orientation. We observed that the DR1P/SWNT film exhibited SHG immediately following fabrication, indicating a degree of chromophore

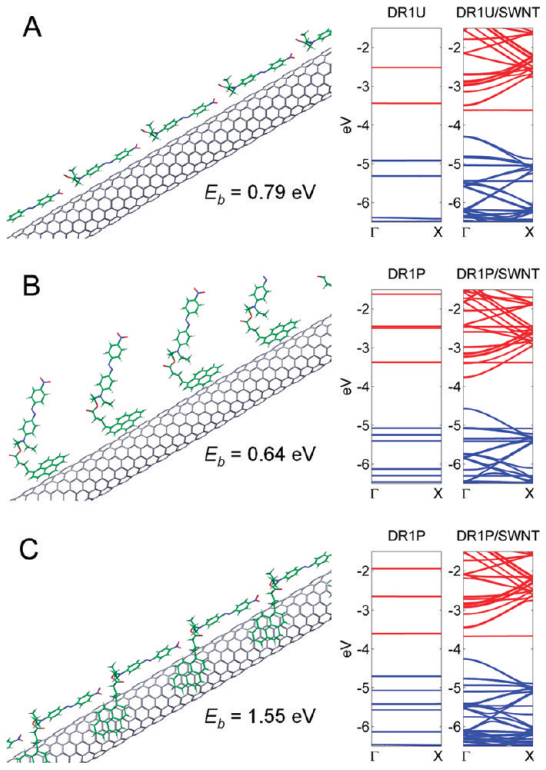

Figure 3. Optimized geometries and electronic band structures of three nanohybrids from DFT calculations using the M06-L/6-31G(d,p) level of theory. The DFT binding energies indicate that DR1P is more strongly adsorbed to the SWNT in the parallel geometry [(C) E_b = 1.55 eV] than in the perpendicular geometry [(B) E_b = 0.64 eV]. If a perpendicular arrangement is assumed, the DR1P is more weakly bound than (unmodified) DR1U [(A) E_b = 0.79 eV]. The band structures of the nanohybrids (last column) show some hybridization between the chromophore with the SWNT, particularly near the X symmetry point. In all three cases, the fundamental band gap of the SWNT is nearly unchanged.

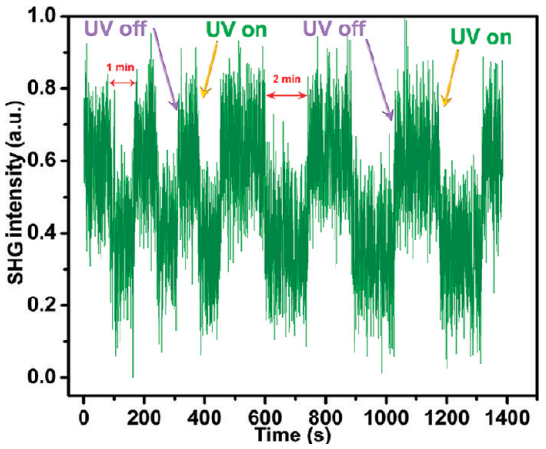

Figure 4. Second harmonic generation (SHG) signal from DR1P/SWNT film subject to cyclic UV irradiation in 1 and 2 min intervals. For example, UV is on for 100 s < t < 160 s, off for 160 s < t < 220 s. At t = 460 s, the period is increased to 2 min.

alignment perpendicular to SWNTs. This SHG signal was not observed for pristine SWNTs. To confirm the role of the chromophores in generation of the SHG signal, further measurements were performed while irradiating the DR1P/SWNT films for 1 min with 365 nm UV light, followed by 1 min without UV light (Figure 4). The DR1P/SWNT film shows a clear dependence of the SHG signal on 365 nm UV light. Upon illumination, the SHG drops noticeably, taking 2−4 s to reach steady state. Following removal of the UV, the SHG returns to its initial value. These results can be repeated for several cycles. The change that occurred during this process was consistent with the isomerization of DR1P oriented in the perpendicular direction. An AmineP/SWNT (Scheme 1) film was prepared as a control as it does not have the switchable azo group. No SHG or dependence on the UV light was observed, confirming the importance of the isomerization of DR1P. Collectively, these results suggest that the adsorption of chromophores on the nanotubes is either heterogeneous (in addition to the parallel configuration of DR1P, there are also perpendicular configurations on the SWNTs) or that the adsorption is at an intermediate angle relative to the axis of the nanotube.

Fluorescence Quenching upon Binding between Chromophores and Nanotubes. The three chromophore samples showed a strong fluorescence emission when not bound to nanotubes (Figure 5). However, in the presence of nanotubes, the fluorescence intensity (F) drops dramatically compared to the initial fluorescence intensity (F_0). For a given concentration of chromophores, as the concentration of nanotubes increases, the emission from the chromophores decreases. The efficiency of quenching ($1 - F/F_0$) for DR1U/SWNTs, DR1A/SWNTs, and DR1P/SWNTs is 84.2, 92.0, and 95.6%, respectively. From the Stern−Volmer plots (F_0/F as a function of nanotube concentration), in moving from DR1U to DR1A to DR1P, an increasing nonlinear plot with a slight upward curvature was observed. The nonlinear plot is typically associated with a combination of both static and dynamic quenching, that is, by both collisions and by complex formation with the chromophores.[30] The absorption spectra of the chromophores with and without SWNTs are presented in Figure 5G−I. The absorption maxima of DR1U, DR1A, and DR1P show red shifts of 5−10 nm upon addition of the SWNTs. The red shift is attributed to changes in energy levels upon binding of the chromophores to the nanotubes and is associated with the static component of quenching mechanism. The interactions between the chromophores and the nanotubes are also supported by the slight upfield shift in the G-band in Raman, upon functionalization with all three chromophores (see Figure 3S in the Supporting Information).[31,32]

The quenching of fluorescence from porphyrins covalently linked to nanotubes has been found to be a function of the length of the linker.[33] In our studies, the length of the linker is 4 and 7 in DR1A and DR1P,

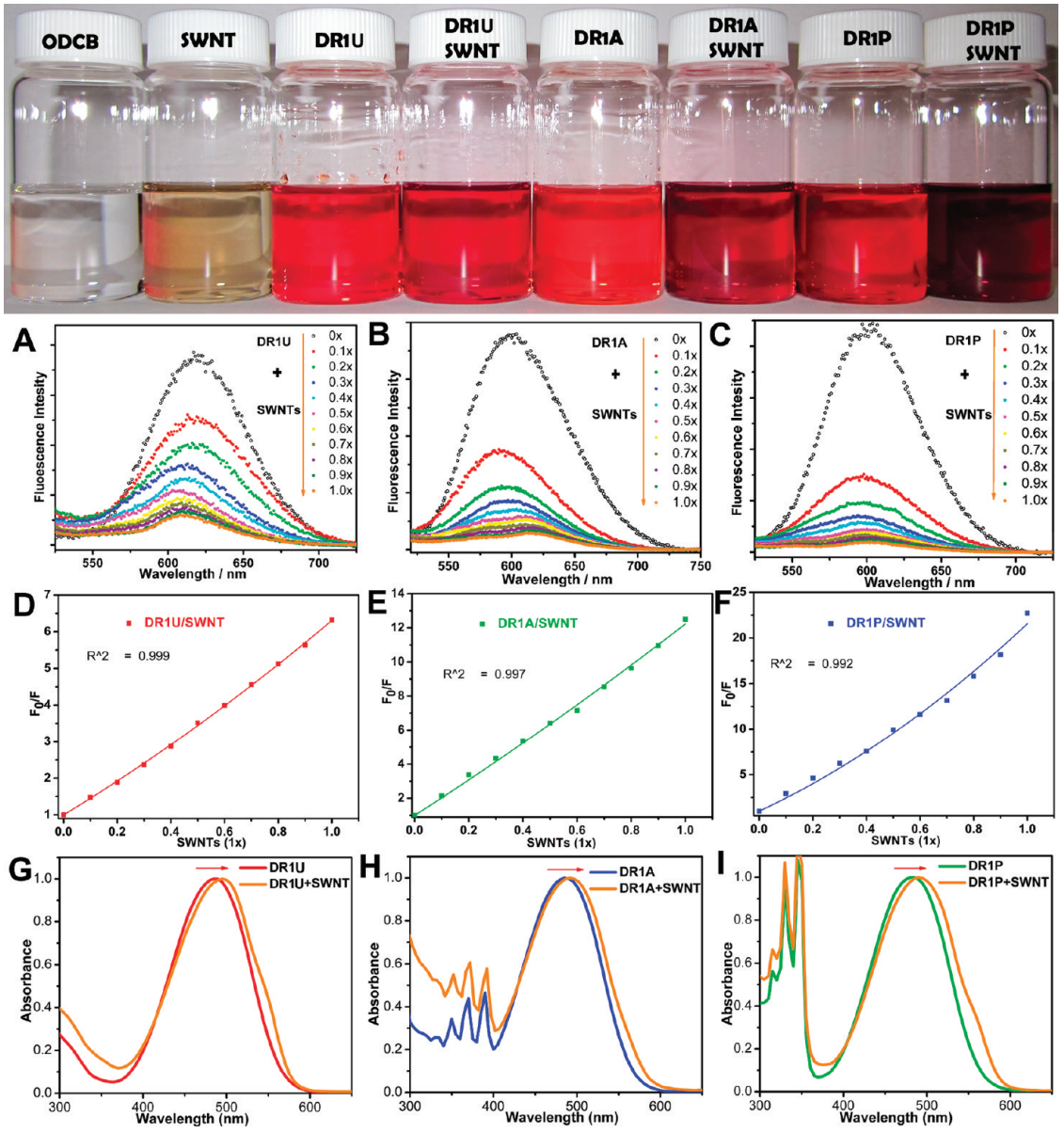

Figure 5. PL spectra after excitation at 490 nm for (A) DR1U, (B) DR1A, and (C) DR1P, show quenching of the fluorescence upon binding. In all three cases, the concentration of the chromophore was fixed at 0.01 mM and the concentration of SWNTs was varied from 0.1× to 1.0×. (D–F) Corresponding Stern–Volmer plots derived from panels A–C, showing increasing nonlinear trends, indicating a combination of static and dynamic quenching. The solid line shows the fit to the nonlinear equation[30] $F_0/F = 1 + b[\text{SWNT}] + c[\text{SWNT}]^2$. Absorption spectrum of (G) DR1U and DR1U/SWNT hybrid, (H) DR1A and DR1A/SWNT hybrid, (I) DR1P and DR1P/SWNT hybrid showing a red shift in the absorption maximum. The top row of labeled photographs shows the prepared solutions.

respectively. Both are reasonably flexible and show equally strong quenching. Hence, the tether length, while important in some cases, does not seem to be critical in our system. The quenching of photoexcited fluorophores by CNTs could be due to energy transfer (*i.e.*, Förster resonant energy transfer), charge transfer (*i.e.*, photoinduced electron transfer), or by metallic nanotubes. We measured the photoluminescence (PL) emission from the nanotubes pumped by absorption of the chromophores (Figure 4S in Supporting Information). The excitation source was 490 nm (close to the λ_{max} of the chromophore), and the chromophore concentration was 5 μM. In all three cases, no detectable enhancement in the band gap PL of nanotubes was observed, which points to a lack of significant energy transfer from the chromophores to isolated semiconducting nanotubes.[31,34–36]

CONCLUSIONS

Three azo-benzene-based chromophores (DR1U, DR1A, and DR1P) were used to study the interaction of chromophores with SWNTs and the effect of the tethers, if present. These experiments highlight the importance of having a strong π–π stacking group such as pyrene

in creating stable nanotube hybrids, while preserving the electronic structure of the nanotubes. Our main conclusions are (a) UV–vis, Raman, and XPS indicate that pyrene forms the strongest tether to nanotubes compared to anthracene or unmodified molecules; (b) DFT calculations show that DR1P with parallel orientation to the nanotube has the largest binding energy; (c) SHG measurements applied for the first time to chromophore-functionalized nanotubes support the presence of a perpendicular component to the overall orientation of DR1P on the SWNTs, suggesting heterogeneous adsorption of the functionalized chromophore; (d) the fluorescence of the dipolar chromophores is quenched upon binding to nanotubes; (e) Stern–Volmer plots are nonlinear, which supports a combination of static and dynamic quenching processes; and (f) PL measurements show no significant energy transfer between the chromophores and the nanotubes. The DFT calculations show that if charge transfer is present it must occur in an excited state. This is relevant for optimizing the photogating of the chromophore/SWNT transistors, and it motivates future work on both tailoring the dipole moment as well as improving the optical activity of the nanotube hybrid material by selecting specific chiral distributions.

METHODS

Chromophore/SWNT Solutions. One milligram of HiPCO-grown SWNTs (Unidym, raw powder) was homogenized in 10 mL of *o*-dichlorobenzene (ODCB) from Sigma-Aldrich in a bath sonicator for 1 h and sonicated by a Fisher Scientific Model 500 sonic dismembrator with a horn tip for 10 min under ambient conditions. ODCB was chosen because nanotubes are highly dispersible in this solvent.[37] These mixtures were subjected to centrifugation (11 000 rpm) for 1.5 h to remove bundles and catalyst residues. The supernatant was centrifuged for an additional 2 h and used as the stock dispersion assuming that the final SWNTs concentration is 1×. Chromophores were added to the SWNT suspensions to obtain a concentration of 0.5 mM. Unmodified Disperse Red 1 (DR1U) (Sigma-Aldrich) was used as received. DR1P and DR1A were synthesized based on a previous literature report.[9]

Chromophore/SWNT Films. Two milliliters of SWNT–chromophore solution was drop-cast onto glass slides (3 in. × 1 in. × 1 mm), dried for 24 h under ambient conditions, and followed by drying in vacuum for 48 h at room temperature. To remove the excess unbound chromophores, the prepared SWNT–chromophore films were dipped into 10 mL of methanol for 30 s and dried under ambient conditions.

Characterization. UV–vis spectra of the hybrids on the glass slides were recorded with a Varian Cary 50 Bio UV–visible spectrophotometer. Fluorescence spectra were taken with an ISS PC1 photon counting fluorometer (ISS Instrument Inc., Champaign, IL) using 490 nm excitation at room temperature. The dispersion and mixing of the solutions were performed just before the measurements. Raman spectra of the hybrids on the glass slides were measured using a Horiba Jobin Yvon LabRAM ARAMIS Raman confocal microscope with 532 nm diode laser excitation.

XPS of the hybrids on the glass slides was measured with a Perkin-Elmer 5400 ESCA spectrometer under Mg Kα X-ray emission. The surface coverages of the chromophores on SWNTs were calculated using standard equations (details in Supporting Information).[38,39]

Second harmonic generation experiments were conducted with a Q-switched 1064 nm pulsed Nd:YAG laser with a 50 mJ pulse energy and 10 ns pulse width. Frequency-doubled light at 532 nm was detected with a photomultiplier and gated boxcar integrating electronics.

Photoluminescence spectra (in the near-infrared range) of SWNTs in *o*-dichlorobenzene and chromophore–SWNTs solution were collected using a high-power LED excitation source at 490 nm and a Horiba Jobin Yvon monochromator with a modulated 4 kHz chopper wheel, calibrated Ge reference cell, and a Stanford Research Systems SR830 lock-in amplifier. The concentration of all three chromophores was fixed at 5 μM and that of SWNTs was 0.05×.

DFT Calculations. Density functional theory (DFT) calculations were performed using the recent M06-L functional, which is designed specifically for noncovalent and π–π stacking interactions.[40] Geometry optimizations for all three chromophores were obtained using the M06-L functional in conjunction with an all-electron 3-21G Gaussian basis set. At the optimized geometries, single-point energies with a larger 6-31G(d,p) basis set were used to calculate final binding energies. To provide further insight into electronic properties, we also computed the electronic band structure at the same M06-L/6-31G(d,p) level of theory for all the SWNT–chromophore hybrids. For all three chromophores, a (10,0) semiconducting SWNT was chosen as a representative model system, and calculations were performed using a one-dimensional supercell along the axis of the nanotube. Since the chromophore molecules are over 6 times longer than the (10,0) unit cell, a large supercell of 17.1 Å along the nanotube axis was chosen to allow separation between adjacent chromophores.

Acknowledgment. P.G. and C.S. acknowledge discussion on XPS with M. Kim and P. Paoprasert; on PL experiments with M.-Y. Wu. We thank J. Burstyn and R. McClain for access to spectroscopic facilities. We acknowledge financial support from the Division of Materials Sciences and Engineering, Office of Basic Energy Science, U.S. Department of Energy under Award #ER46590. D.J.M. acknowledges support from NSF-DMR Award #1138416. B.M.W. and F.L. acknowledge support from the Laboratory Directed Research and Development program at Sandia National Laboratories, a multiprogram laboratory operated by Sandia Corporation, a Lockheed Martin Company, for the United States Department of Energy under Contract DE-AC04-94-AL85000.

Supporting Information Available: UV–vis spectra of the three hybrids before and after washing with methanol, Raman spectra of the three chromophores and the hybrids, XPS calculations for coverages, and PL spectrum of the three hybrids. This material is available free of charge *via* the Internet at http://pubs.acs.org.

REFERENCES AND NOTES

1. Komarov, V. M.; Kayushin, L. P. Nature of the Primary Photochemical Act of Mechanism of Vision 1. Chromophore Rhodopsin Center - Spectral-Luminescent Properties. *Stud. Biophys.* **1975**, *52*, 107–140.
2. Darwin, C. *The Power of Movement in Plants*; Murray: London, 1880.
3. Schoenlein, R.; Peteanu, L.; Mathies, R.; Shank, C. The First Step in Vision: Femtosecond Isomerization of Rhodopsin. *Science* **1991**, *254*, 412–415.
4. Crescitelli, F. The Natural History of Visual Pigments: 1990. *Prog. Retinal Eye Res.* **1991**, *11*, 1–32.

5. Barrett, C. J.; Mamiya, J.; Yager, K. G.; Ikeda, T. Photomechanical Effects in Azobenzene-Containing Soft Materials. *Soft Matter* **2007**, *3*, 1249–1261.
6. Das, B.; Abe, S. Molecular Switch on a Metal Surface. *J. Phys. Chem. B* **2006**, *110*, 4247–4255.
7. Wen, Y.; Yi, W.; Meng, L.; Feng, M.; Jiang, G.; Yuan, W.; Zhang, Y.; Gao, H.; Jiang, L.; Song, Y. Photochemical-Controlled Switching Based on Azobenzene Monolayer Modified Silicon (111) Surface. *J. Phys. Chem. B* **2005**, *109*, 14465–14468.
8. Yasuda, S.; Nakamura, T.; Matsumoto, M.; Shigekawa, H. Phase Switching of a Single Isomeric Molecule and Associated Characteristic Rectification. *J. Am. Chem. Soc.* **2003**, *125*, 16430–16433.
9. Simmons, J. M.; In, I.; Campbell, V. E.; Mark, T. J.; Léonard, F.; Gopalan, P.; Eriksson, M. A. Optically Modulated Conduction in Chromophore-Functionalized Single-Wall Carbon Nanotubes. *Phys. Rev. Lett.* **2007**, *98*, 086802.
10. Freitag, M.; Martin, Y.; Misewich, J. A.; Martel, R.; Avouris, P. Photoconductivity of Single Carbon Nanotubes. *Nano Lett.* **2003**, *3*, 1067–1071.
11. Zhou, X.; Zifer, T.; Wong, B. M.; Krafcik, K. L.; Léonard, F.; Vance, A. L. Color Detection Using Chromophore–Nanotube Hybrid Devices. *Nano Lett.* **2009**, *9*, 1028–1033.
12. Kolpak, A. M.; Grossman, J. C. Azobenzene-Functionalized Carbon Nanotubes as High-Energy Density Solar Thermal Fuels. *Nano Lett.* **2011**, *11*, 3156–3162.
13. Feng, Y.; Zhang, X.; Ding, X.; Feng, W. A Light-Driven Reversible Conductance Switch Based on a Few-Walled Carbon Nanotube/Azobenzene Hybrid Linked by a Flexible Spacer. *Carbon* **2010**, *48*, 3091–3096.
14. Zhao, Y. -L.; Stoddart, J. F. Noncovalent Functionalization of Single-Walled Carbon Nanotubes. *Acc. Chem. Res.* **2009**, *42*, 1161–1171.
15. Vijayakumar, C.; Balan, B.; Kim, M. J.; Takeuchi, M. Noncovalent Functionalization of SWNTs with Azobenzene-Containing Polymers: Solubility, Stability, and Enhancement of Photoresponsive Properties. *J. Phys. Chem. C* **2011**, *115*, 4533–4539.
16. Chen, R. J.; Zhang, Y.; Wang, D.; Dai, H. Noncovalent Sidewall Functionalization of Single-Walled Carbon Nanotubes for Protein Immobilization. *J. Am. Chem. Soc.* **2001**, *123*, 3838–3839.
17. D'Souza, F.; Chitta, R.; Sandanayaka, A. S. D.; Subbaiyan, N. K.; D'Souza, L.; Araki, Y.; Ito, O. Supramolecular Carbon Nanotube–Fullerene Donor–Acceptor Hybrids for Photoinduced Electron Transfer. *J. Am. Chem. Soc.* **2007**, *129*, 15865–15871.
18. Lu, J.; Nagase, S.; Zhang, X.; Wang, D.; Ni, M.; Maeda, Y.; Wakahara, T.; Nakahodo, T.; Tsuchiya, T.; Akasaka, T.; *et al.* Selective Interaction of Large or Charge-Transfer Aromatic Molecules with Metallic Single-Wall Carbon Nanotubes: Critical Role of the Molecular Size and Orientation. *J. Am. Chem. Soc.* **2006**, *128*, 5114–5118.
19. Rao, A. M.; Richter, E.; Bandow, S.; Chase, B.; Eklund, P. C.; Williams, K. A.; Fang, S.; Subbaswamy, K. R.; Menon, M.; Thess, A.; *et al.* Diameter-Selective Raman Scattering from Vibrational Modes in Carbon Nanotubes. *Science* **1997**, *275*, 187–191.
20. Moonoosawmy, K. R.; Kruse, P. To Dope or Not To Dope: The Effect of Sonicating Single-Wall Carbon Nanotubes in Common Laboratory Solvents on Their Electronic Structure. *J. Am. Chem. Soc.* **2008**, *130*, 13417–13424.
21. Biswas, N.; Umapathy, S. Resonance Raman Study of the Solvent Dynamics for Ultrafast Charge Transfer Transition in 4-Nitro-4′-dimethylamino-Azobenzene. *J. Chem. Phys.* **2003**, *118*, 5526–5536.
22. Rao, A. M.; Bandow, S.; Richter, E.; Eklund, P. C. Raman Spectroscopy of Pristine and Doped Single Wall Carbon Nanotubes. *Thin Solid Films* **1998**, *331*, 141–147.
23. Okpalugo, T. I. T.; Papakonstantinou, P.; Murphy, H.; McLaughlin, J.; Brown, N. M. D. High Resolution XPS Characterization of Chemical Functionalised MWCNTs and SWCNTs. *Carbon* **2005**, *43*, 153–161.
24. Wong, B. M. Noncovalent Interactions in Supramolecular Complexes: A Study on Corannulene and the Double Concave Buckycatcher. *J. Comput. Chem.* **2009**, *30*, 51–56.
25. Zhao, Y.; Truhlar, D. G. Size-Selective Supramolecular Chemistry in a Hydrocarbon Nanoring. *J. Am. Chem. Soc.* **2007**, *129*, 8440–8442.
26. Shen, Y. R. Optical 2nd Harmonic-Generation at Interfaces. *Annu. Rev. Phys. Chem.* **1989**, *40*, 327–350.
27. Simpson, G. J.; Rowlen, K. L. Measurement of Orientation in Organic Thin Films. *Acc. Chem. Res.* **2000**, *33*, 781–789.
28. Loucifsaibi, R.; Nakatani, K.; Delaire, J. A.; Dumont, M.; Sekkat, Z. Photoisomerization and 2nd Harmonic-Generation in Disperse Red One-Doped and Functionalized Poly-(methyl methacrylate) Films. *Chem. Mater.* **1993**, *5*, 229–236.
29. Zyss, J.; Chemla, D. S. *Nonlinear Optical Properties of Organic Molecules and Crystals*; Academic Press: Orlando, FL, 1987; Vol. 1.
30. Lakowicz, J. R. *Principles of Fluorescence Spectroscopy*; Springer Science: New York, 2006.
31. Ahmad, A.; Kern, K.; Balasubramanian, K. Selective Enhancement of Carbon Nanotube Photoluminescence by Resonant Energy Transfer. *ChemPhysChem* **2009**, *10*, 905–909.
32. Zhu, Z.; Yang, R.; You, M.; Zhang, X.; Wu, Y.; Tan, W. Single-Walled Carbon Nanotube as an Effective Quencher. *Anal. Bioanal. Chem.* **2010**, *396*, 73–83.
33. Li, H.; Martin, R. B.; Harruff, B. A.; Carino, R. A.; Allard, L. F.; Sun, Y. P. Single-Walled Carbon Nanotubes Tethered with Porphyrins: Synthesis and Photophysical Properties. *Adv. Mater.* **2004**, *16*, 896–900.
34. Dettlaff-Weglikowska, U.; Skákalová, V.; Graupner, R.; Jhang, S. H.; Kim, B. H.; Lee, H. J.; Ley, L.; Park, Y. W.; Berber, S.; Tománek, D.; *et al.* Effect of $SOCl_2$ Treatment on Electrical and Mechanical Properties of Single-Wall Carbon Nanotube Networks. *J. Am. Chem. Soc.* **2005**, *127*, 5125–5131.
35. Kim, K. K.; Bae, J. J.; Park, H. K.; Kim, S. M.; Geng, H.-Z.; Park, K. A.; Shin, H.-J.; Yoon, S.-M.; Benayad, A.; Choi, J.-Y.; *et al.* Fermi Level Engineering of Single-Walled Carbon Nanotubes by $AuCl_3$ Doping. *J. Am. Chem. Soc.* **2008**, *130*, 12757–12761.
36. Zhou, W.; Vavro, J.; Nemes, N. M.; Fischer, J. E.; Borondics, F.; Kamarás, K.; Tanner, D. B. Charge Transfer and Fermi Level Shift in p-Doped Single-Walled Carbon Nanotubes. *Phys. Rev. B* **2005**, *71*, 205423.
37. Bahr, J. L.; Mickelson, E. T.; Bronikowski, M. J.; Smalley, R. E.; Tour, J. M. Dissolution of Small Diameter Single-Wall Carbon Nanotubes in Organic Solvents? *Chem. Commun.* **2001**, 193–194.
38. Kim, H.; Colavita, P. E.; Paoprasert, P.; Gopalan, P.; Kuech, T. F.; Hamers, R. J. Grafting of Molecular Layers to Oxidized Gallium Nitride Surfaces *via* Phosphonic Acid Linkages. *Surf. Sci.* **2008**, *602*, 2382–2388.
39. Paoprasert, P.; Spalenka, J. W.; Peterson, D. L.; Ruther, R. E.; Hamers, R. J.; Evans, P. G.; Gopalan, P. Grafting of Poly-(3-hexylthiophene) Brushes on Oxides Using Click Chemistry. *J. Mater. Chem.* **2010**, *20*, 2651–2658.
40. Zhao, Y.; Truhlar, D. G. Density Functionals with Broad Applicability in Chemistry. *Acc. Chem. Res.* **2008**, *41*, 157–167.